Remote Sensing of Cloud Properties with Lidar and Radiometry

C. M. R. Platt[1], S. A. Young, and R. T. Austin[1]

CSIRO, Division of Atmospheric Research, Aspendale, Victoria, Australia.
1. Now at Atmospheric Science, Colorado State University, Fort Collins, CO, 80523, USA

1. Groundbased observations of clouds.

The remote sensing of cloud structural and optical properties by groundbased lidar and radiometry has been developed over a number of years, particularly at the CSIRO Division of Atmospheric Research, Aspendale, Australia (1,2). The results obtained from groundbased sensing can be used to simulate realistically the backscatter and infrared (IR) emittance properties that can be expected from space lidar observations.

Detailed information can be obtained from cloud remote sensing from the surface with lidar and IR radiometry-the Lidar/Radiometer (LIRAD) method. The ultimate aim of the experiments is to understand the radiative divergence in clouds that leads both to direct heating or cooling of atmospheric layers remote from the surface and to a change in outgoing radiation at the top of the atmosphere. These processes are important issues in climate prediction, but are not yet fully understood.

The LIRAD generates two pieces of information, being the cloud optical depths at wavelengths in the IR and visible spectrum respectively. Utilizing well understood spectral variations in the refractive index properties of water or ice, and making some assumptions on particle size distributions and shape, the cloud spectral optical properties, and thus total cloud heating, can then be calculated. As the solar absorption in the cloud, which is also an important factor, depends on cloud particle size, a number size spectrum also has to be assumed. However, this can be estimated from size distribution information collated from aircraft and balloon in situ measurements (3). This additional information can also be obtained by operating millimeter radar coincident with LIRAD observations (4,5). Lidar sounding also gives a measure of inhomogeneities in the cloud, which can now be treated analytically in the calculation of cloud heating rates (e.g., 6).

In the LIRAD analysis, the effects of water vapour absorption and emission are first removed by experimental and theoretical methods (1). A relation can then be derived that relates the calculated lidar attenuated integrated backscatter $\gamma'(\pi)$ to the retrieved IR emittance, ε_a:

$$\gamma'(\pi) = \frac{k}{2\eta}\left[1 - \exp(-2\eta\alpha \log\frac{1}{1-\varepsilon_a})\right], \qquad (1)$$

where k is the cloud particle backscatter to extinction ratio, η is a multiple scattering factor and α is the ratio of visible optical depth δ_c to IR optical depth δ_a.

Observations have been made on mid-latitude (2), tropical, and equatorial cirrus (7), and mid-level mixed-phase mid-latitude clouds (8). Examples of cirrus time - height images are shown in Figure 1. Plots of $\gamma'(\pi)$ versus ε_a for the same clouds are shown in Figure 2. They follow the form of equation 1 but with different amounts of scatter (2). The scatter is larger for mixed-phase clouds than for cirrus clouds. Values of $k/2\eta$ $(= \gamma'(\pi), \varepsilon_a \rightarrow 1)$, when corrected for multiple scattering, indicate changes in backscatter phase function, which is related to the cloud particle habit. Values of α (retrieved from the shape of Eq. 1) give information on cloud particle size (1).

Values of cloud properties in the various regions and at various temperatures have been collated in (7). Plots of $k/2\eta$ and ε_a against mid-cloud temperature are shown in Figures 3 and 4 respectively. These comparisons show that both quantities are related to temperature, which is perhaps not surprising. It also points to the possibility of parameterizing cloud properties in terms of temperature.

The above observations and analyses circumvent the necessity for determining the cloud microphysics *per se,* so far as calculating the heating functions of the clouds is concerned. However, to obtain a complete statistical picture for cloud modeling purposes, and to estimate cloud absorption, cloud particle size distributions in different types of clouds and at different temperatures are still needed.

2. Implications for space lidar.

It is interesting to consider the different sampling strategies between groundbased and spacebased lidar. In the former case, spatial sampling is poor, or non-existent whereas temporal sampling is determined by the total time in which observations are made. The opposite is true of sampling from space, where spatial sampling is good, but temporal sampling is generally limited. In both cases, statistical properties of the clouds can be obtained.

Bearing in mind these differences, similar observations to LIRAD can be made from space. The requirement is for a radiometer flown together with a lidar, both viewing in the nadir. The radiometer could be a type of imager that has flown previously on both geostationary and polar orbiting satellites.

IR emittances can thus be retrieved with a LIRAD-type observation from space. For that case, the upwelling radiance below the cloud needs to be measured or calculated, but, at least for cirrus, the water vapor absorption will be zero. A retrieval method for IR emittance is shown schematically in Figure 5. It is obviously more accurate to retrieve IR emittance over ocean areas where surface temperature is less variable than over land, or alternatively where there are lower clouds. However, lidar will enable a measure of radiance below the cloud, even in the presence of lower clouds, if the lower cloud height can be measured and atmospheric temperature profiles are available. Such temperatures are in any case necessary for the LIRAD retrieval and can be obtained from global forecast assimilation temperature profiles. Work on such retrievals has been done previously using aircraft data. Measured solar reflectance and IR emittance were compared (9).

3. Acknowledgments.

The authors wish to acknowledge the major contributions of their colleagues at the CSIRO, Division of Atmospheric Research, Aspendale, Australia. Part of this work was supported by the U. S. Department of Energy, Office of Health and Environmental Research, Grant No. DE-FG02-92ER61373.

4. References

1. Platt, C. M. R., 1979: Remote sounding of high clouds: I. Calculation of visible and infrared properties from lidar and radiometer measurements. *J. Appl. Meteor.*, **18**, 1130-1143.

2. Platt, C. M. R., J. C. Scott and A. C. Dilley, 1987: "Remote sounding of high clouds. Part VI: Optical properties of midlatitude and tropical cirrus." *J. Atmos. Sci..*, **44**, 729-747.

3. Platt, C. M. R., 1997: A parameterization of the visible extinction coefficient of ice clouds in terms of the ice water/content *J. Atmos. Sci.*, **54**, 2083-2098.

4. Intrieri, J. M., G. L. Stephens, W. L. Eberhard and T. Uttal, 1993: A method for determining cirrus cloud particle sizes using lidar and radar backscatter technique. *J. Appl. Meteor.*, **32**, 1074-1082.

5. Matrosov, S. Y., T. Uttal, J. B. Snider, and R. A. Kropfli, 1992: Estimation of ice cloud parameters from ground-based infrared radiometer and radar measurements. *J. Geophys. Res.*, **97**, 11,567-11,574.

6. Evans, K. F., 1993: two-dimensional radiative transfer in cloudy atmospheres; the spherical harmonic spatial grid method. *J. Atmos. Sci.*, **50**, 3111-3124.

7. Platt, C. M. R., S. A. Young, P. J. Manson, G. R. Patterson, S. C. Marsden, R. T. Austin, and J. H. Churnside, 1998: The optical properties of tropical cirrus in the ARM Pilot Radiation Observation Experiment. *J. Atmos. Sci.*, (In press)

8. Young, S. A., C. M. R. Platt, R. T. Austin, and G. R. Patterson, 1998: Optical properties and microphysics of some mid-latitude, mid-level clouds in ECLIPS. Submitted to *J. Appl. Met.*

9. Spinhirne, J. D., W. D. Hart and D. L. Hlavka, 1996: Cirrus infrared parameters and shortwave reflectance relations from observations. *J. Atmos. Sci.*, **53**, 1438 - 1458.

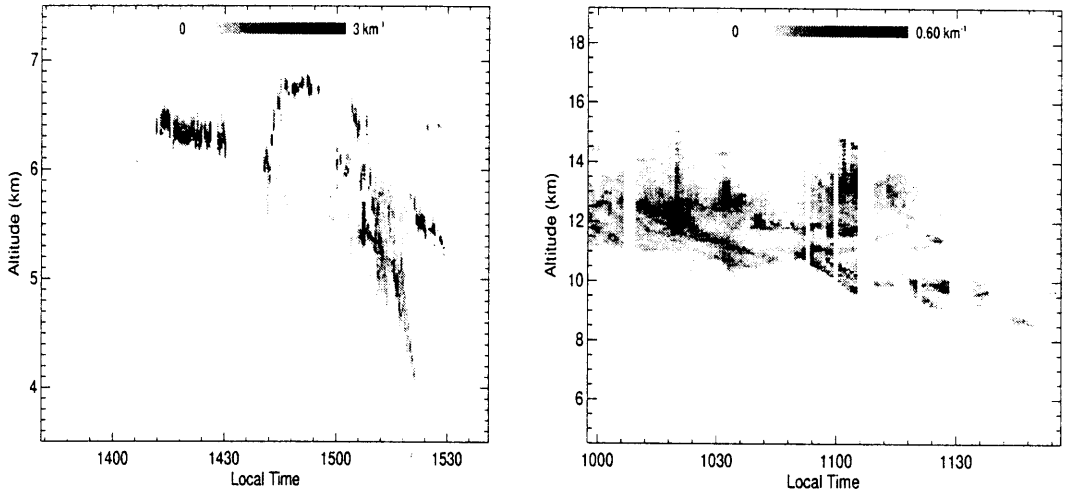

Figure 1: Time-height images of lidar backscatter. Left, for a mid-level mixed phase cloud. Right, for a high tropical cirrus cloud.

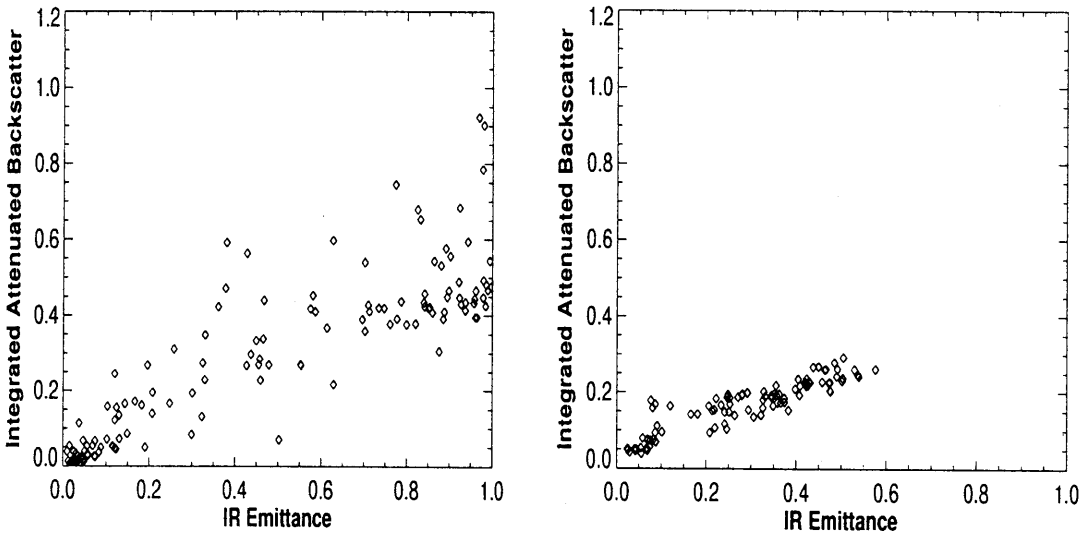

Figure 2. Plot of integrated attenuated backscatter $\gamma'(\pi)$ versus IR emittance ε_a. Left, for the cloud in Figure 1(left). Right, for the cloud in Figure 1(Right).

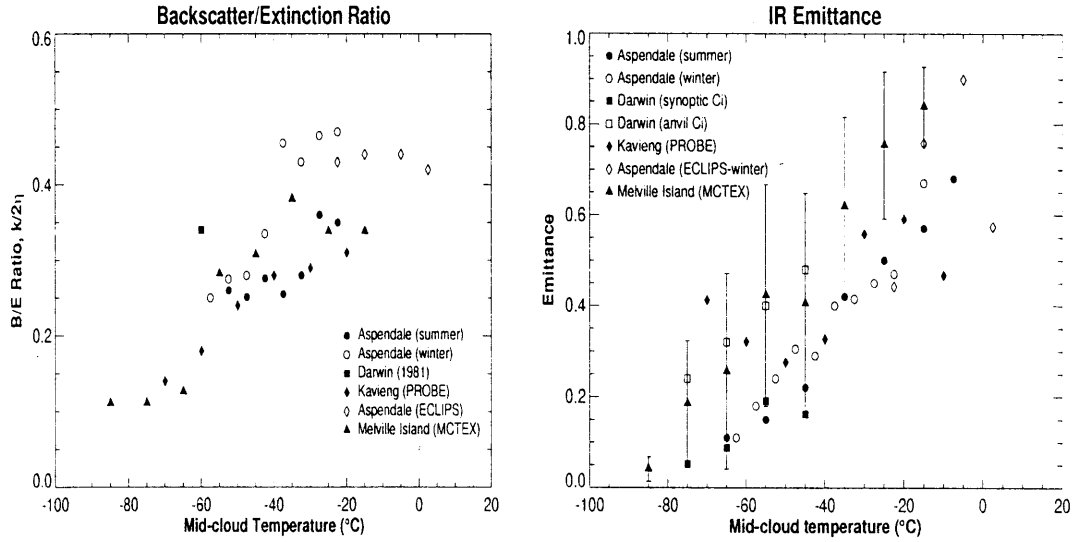

Figure 3. Plots of: Left, the effective backscatter to extinction ratio $k / 2\eta$ against mid-cloud temperature, Right, The infrared emittance ε_a against mid-cloud temperature, for several different field expeditions. Aspendale summer and winter are from (2), Darwin from Platt et al., 1984, *J. Clim. Appl. Meteor.*, **23**, 1296-1308. Kavieng PROBE from (7). Aspendale ECLIPS and Melville Island MCTEX are in preparation.

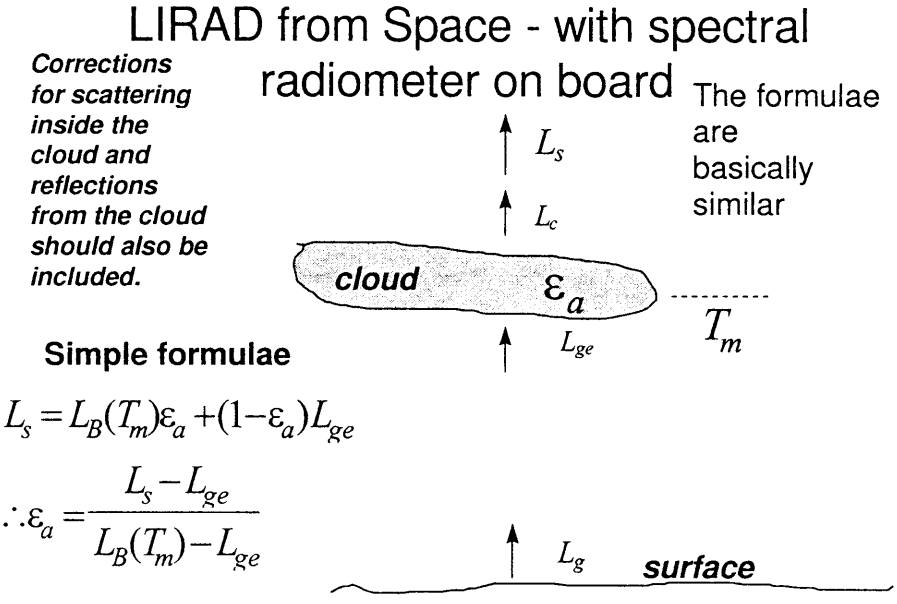

Figure 5. Schematic of a retrieval of cirrus emittance ε_a from upwelling radiance L_c (=L_s) at cloud top and L_{ge} below the cloud base. $L_b(T_m)$ is the filter radiometer blackbody radiance at cloud temperature.